Lithium Secondary Batteries Using Modified-Imidazolium Room-Temperature Ionic Liquid

9 AUTHORS, INCLUDING:

Shiro Seki

Central Research Institute of Electric Power I…

73 PUBLICATIONS **2,189** CITATIONS

SEE PROFILE

Y. Kobayashi

Central Research Institute of Electric Power I…

71 PUBLICATIONS **2,373** CITATIONS

SEE PROFILE

Yuichi Mita

Central Research Institute of Electric Power I…

34 PUBLICATIONS **1,087** CITATIONS

SEE PROFILE

Masayoshi Watanabe

Yokohama National University

350 PUBLICATIONS **14,344** CITATIONS

SEE PROFILE

Lithium Secondary Batteries Using Modified-Imidazolium Room-Temperature Ionic Liquid

**Shiro Seki,*,†,‡ Yo Kobayashi,† Hajime Miyashiro,† Yasutaka Ohno,§ Akira Usami,†
Yuichi Mita,† Nobuo Kihira,† Masayoshi Watanabe,‡ and Nobuyuki Terada†**

*Materials Science Research Laboratory, Central Research Institute of Electric Power Industry (CRIEPI),
2-11-1, Iwado-kita, Komae, Tokyo 201-8511, Japan, Electric Power Engineering Systems Company Limited,
2-11-1, Iwado-kita, Komae, Tokyo 201-8511, Japan, and Department of Chemistry and Biotechnology,
Yokohama National University, 79-5 Tokiwadai, Hodogaya-ku, Yokohama, Kanagawa 240-8501, Japan*

Received: April 4, 2006; In Final Form: April 28, 2006

Highly reversible, safe lithium secondary batteries that use imidazolium-cation-based room-temperature ionic liquid as an electrolyte and lithium metal as an anode material were realized by the molecular design. To achieve higher reduction stability, an electron-donating substituent was introduced to promote charge delocalization in the imidazolium cation of room-temperature ionic liquids.

Introduction

The realization of large-scale electrochemical devices is strongly expected all over the world, owing to the demand for energy storage devices, for example, load-leveling systems. Although batteries, such as the sodium−sulfur battery and redox-flow battery, have been in practical use as megawatt-class, large-scale batteries up to now, there has been much concern regarding lithium secondary batteries for the purpose of achieving high-energy-density and maintenance-free battery systems.[1] Although safety is very important in the case of large-scale battery systems, flammable aprotic organic solvents are generally used for electrolyte solutions. However, a lithium secondary battery that uses room-temperature ionic liquid as an electrolyte has recently been examined.[2−11] Ionic liquids are nonflammable and nonvolatile because they consist only of cations and anions[12] and are promising electrolytes for use in large-scale lithium secondary batteries.

Although there have been a lot of research studies concerning ionic liquids that use imidazolium-based cations (for example, synthesis solvent and catalysis),[13] the problem of a stability limit up to the redox potential of lithium metal has been pointed out, and there have been very few reports on rechargeable batteries that use lithium metal as an anode.[14] In this research study, we examined the battery characteristics of lithium metal secondary batteries using an ionic liquid that introduced an electron-donating substituent at the second position of the imidazolium cation and a long alkyl chain at the third position to promote charge delocalization in the imidazolium cation and to improve the reduction stability of imidazolium-based ionic liquids. We aimed to realize a battery system that has both safety and high performance by the molecular design of the room-temperature ionic liquid.
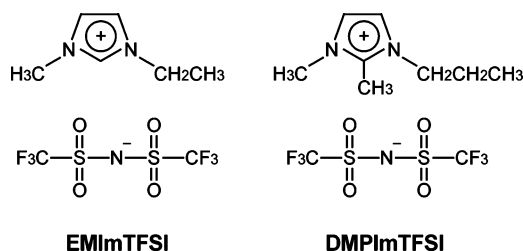

Figure 1. Chemical structures of EMImTFSI and DMPImTFSI.

Experimental Section

1-Ethyl-3-methylimidazolium bis(trifluoromethylsulfonyl)-imide (EMImTFSI) and 1,2-dimethyl-3-propylimidazolium bis-(trifluoromethylsulfonyl)imide (DMPImTFSI) were used as room-temperature ionic liquids (Aldrich-Fluka), as shown in Figure 1. These ionic liquids were dried in a vacuum at 323 K for more than 24 h and stored in a dry-argon-filled glovebox ($[O_2] < 0.4$ ppm, $[H_2O] < 0.1$ ppm, Miwa MFG Co., Ltd.). Ionic liquid−lithium salt (lithium bis(trifluoromethanesulfonyl)-imide, LiTFSI, Kishida Chemical Co., LTD) mixture electrolytes were prepared by dissolving the given amounts (LiTFSI concentration is 0.32 mol kg^{-1}, molar ratio of [room-temperature ionic liquid cation]/[lithium cation] is approximately 7) of ionic liquid and lithium salt, and stilled at room temperature.

The temperature dependences of ionic conductivity (σ) for the bulk ionic liquids and ionic liquid−lithium salt mixture electrolytes were measured using SUS (stainless steel)/electrolyte/SUS cells and determined by the complex impedance method, using an AC impedance analyzer (Princeton Applied Research, PARSTAT-2263, 200 kHz−50 mHz; impressed voltage 10 mV) at temperatures between 353 and 233 K with cooling processes. Battery characteristics were examined using LiCoO$_2$ cathode/ionic liquid−lithium salt mixture electrolytes/lithium metal anode cells. The cathode sheet consisted of LiCoO$_2$ (85 wt %) as a cathode-active material, acetylene black (9 wt %, Denki Kagaku Kogyo) as an electrically conductive additive, and poly-(vinylidene fluoride) (PVDF, 6 wt %, Kureha Chemical) as a

* To whom correspondence should be addressed. E-mail: s-seki@criepi.denken.or.jp. Fax: +81-3-3480-3401. Phone: +81-3-3480-2111.
† Central Research Institute of Electric Power Industry (CRIEPI).
‡ Yokohama National University.
§ Electric Power Engineering Systems Company Limited.

Letters

J. Phys. Chem. B, Vol. 110, No. 21, 2006 **10229**
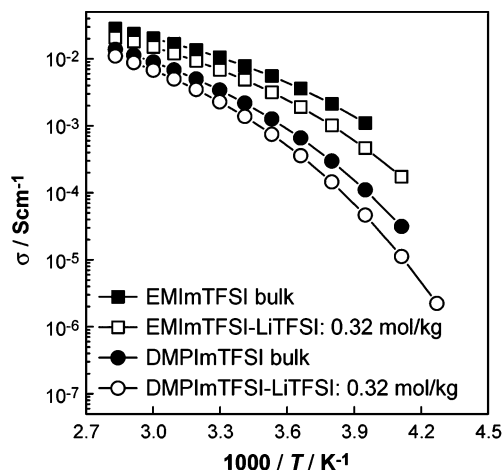
Figure 2. Arrhenius plots of ionic conductivity (σ) for the EMImTFSI, DMPImTFSI, EMImTFSI−LiTFSI mixture electrolyte, and DMPImTFSI−LiTFSI mixture electrolyte.

binder polymer. These constituent materials were thoroughly agitated together in a homogenizer. The obtained paste was applied onto an aluminum current collector using an automatic applicator. After drying the cathode paste, the cathode sheet was compressed to increase packing density and to improve electrical conductivity. The cathode sheet, separator, ionic liquid−lithium salt mixture electrolytes, and lithium metal anode (Honjo Metal, 2 cm^2 area, 300 μm thick) were encapsulated into 2032-type coin cells. The weight ratio of the LiCoO$_2$ cathode/lithium metal anode was approximately 1:3, and the molecular ratio of the LiCoO$_2$ cathode/lithium metal anode was approximately 1:45, respectively. Charge−discharge cycle-life tests of the cells were performed at 3.0−4.2 V with a current density of 0.05 mA cm^{-2} ($^1/_8$ C) at room temperature (constant current charge − constant current discharge). Charge−discharge rate-performance tests were performed at 3.0−4.2 V with current densities of 0.05 mA cm^{-2} (constant current charge) and 0.05, 0.10 ($^1/_4$ C), 0.20 ($^1/_2$ C), and 0.40 mA cm^{-2} (1 C) at 303 K (constant current discharge).

Results and Discussion

Figure 2 shows the temperature dependences of ionic conductivity (σ) for the EMImTFSI bulk, DMPImTFSI bulk, EMImTFSI−LiTFSI mixture electrolyte, and DMPImTFSI−LiTFSI mixture electrolyte used in this study (the response frequency was on the kilohertz order). All plots indicate the Vogel−Tamman−Fulcher (VTF)-type temperature dependence. The values of σ for EMImTFSI and DMPImTFSI at 303 K were 1.06×10^{-2} and 3.41×10^{-3} S cm^{-1}, respectively. The value of σ for DMPImTFSI was approximately one-third that of EMImTFSI. The cause of the difference in the σ values between EMImTFSI and DMPImTFSI electrolytes might have been because of a viscosity increase due to friction between molecules and an increase in molecular weight. Although the σ values were slightly decreased when LiTFSI was added, a higher ionic conductivity ($>10^{-3}$ S cm^{-1}) was obtained, and therefore, a high applicability of room-temperature ionic liquids as electrolytes for lithium secondary batteries is expected.

Moreover, the Arrhenius plots of ionic conductivity for all electrolytes exhibit positively curved profiles, necessitating further interpretation of the results by either the Williams−Landel−Ferry (WLF) or the VTF equation. We applied the VTF equation for the ionic conductivity[15−17]

$$\sigma = AT^{-1/2} \exp[-B/(T - T_0)] \tag{1}$$

where A is a pre-exponential constant proportional to the number of carrier ions in the case of infinitely high temperature, B is the pseudoactivation energy for conduction, and T_0 is the ideal glass transition temperature. Table 1 shows the calculated VTF parameter values for various electrolytes. Adding LiTFSI to both EMImTFSI and DMPImTFSI systems causes an increase in A. The numbers of carrier ions (in this study, EMIm or DMPIm cations, TFSI anions, and lithium cations) might increase by adding LiTFSI, that is, by dissociation of LiTFSI. B increases with LiTFSI addition, and this correlates with inclinations in the Arrhenius plots (significant decrease of σ at low temperature). There is little change in T_0, which is assumed to be the temperature at which ionic transport freezes.

TABLE 1: VTF Equation ($\sigma = AT^{-1/2} \exp[-B/(T - T_0)]$) Parameters for Ionic Conductivity Data for EMImTFSI, DMPImTFSI, EMImTFSI−LiTFSI Mixture Electrolyte, and DMPImTFSI−LiTFSI Mixture Electrolyte

electrolyte	A (S m^{-1} K$^{1/2}$)	B (10^2 K)	T_0 (10^2 K)	R^2 (10^{-1})
EMITFSI bulk	0.161 ± 0.010	6.28 ± 0.17	1.63 ± 0.02	9.99
EMImTFSI/LiTFSI	0.174 ± 0.001	6.78 ± 0.11	1.68 ± 0.01	9.99
DMPImTFSI bulk	0.241 ± 0.013	8.04 ± 0.12	1.71 ± 0.01	9.99
DMPImTFSI/LiTFSI	0.348 ± 0.029	9.13 ± 0.18	1.70 ± 0.01	9.99

Because the ionic conductivity of the imidazolium-based ionic liquid electrolytes is high compared with those of quaternary ammonium-based ionic liquids that have been examined to date,[7,10] their basic characteristics as battery electrolytes and the effects of the methyl group at the second position and the long alkyl chain at the third position in the imidazolium cation were examined. Figure 3a shows the cycle-number dependence of the cathode-limited discharge capacity of the cells with EMImTFSI and DMPImTFSI as the electrolytes. The initial discharge capacities of the EMImTFSI battery and the DMPImTFSI battery were 124 and 130 mA h g^{-1}, respectively, which are slightly smaller than the theoretical capacity of Li$_x$CoO$_2$ (0.5 < x < 1). For the EMImTFSI battery, the discharge capacity became 107 mA h g^{-1} after 50 cycles (86% of the initial capacity), whereas the DMPImTFSI battery maintained 121 mA h g^{-1} (93% of the initial capacity). Figure 3b shows the cycle-number dependence of the Coulombic efficiency, calculated from the charge capacity and discharge capacity. The Coulombic efficiency had high and constant values of 96% (EMImTFSI) and more than 99.5% (DMPImTFSI) after several cycles. The improvement of reversibility was confirmed upon introducing the electron-releasing methyl group at the second position of the imidazolium cation and the longer propyl group at the third position. In particular, in the case of the EMIm cation, it is expected that the high reactivity of the hydrogen at the second position leads to a low reduction stability; therefore, the investigation for which Li$_4$Ti$_5$O$_{12}$ (redox potential is 1.5 V higher than that of Li/Li$^+$) was used as an anode material was reported.[3,4] Substituting the chemically stable methyl group reduces the high reactivity; this might have controlled the side reaction with the metallic lithium anode. Without causing excrescent side reactions other than the charge−discharge (oxidation−reduction) reactions of the LiCoO$_2$ cathode and lithium metal anode, a high reversibility was achieved in the battery systems that used the imidazolium-based room-temperature ionic liquids.

The output characteristic of the battery (rate performance) is also an important factor for the practical use of the ionic liquid lithium batteries as well as the cycle performance. Figure 4
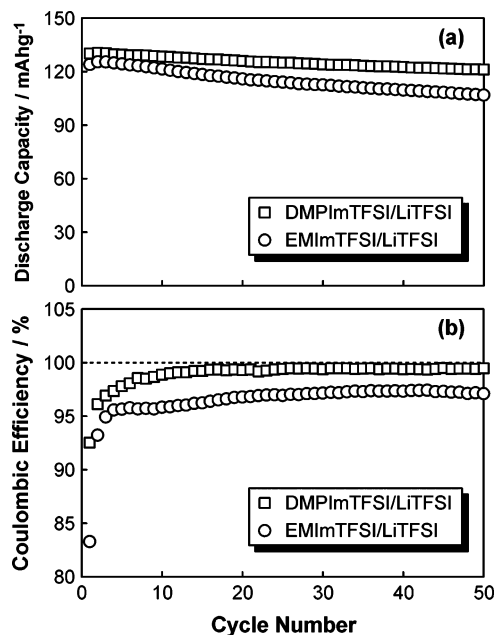
Figure 3. Cycle-life performances for LiCoO$_2$ cathode|EMImTFSI−LiTFSI mixture electrolyte and DMPImTFSI−LiTFSI mixture electrolyte|lithium metal anode cells: (a) discharge capacity; (b) Coulombic efficiency.
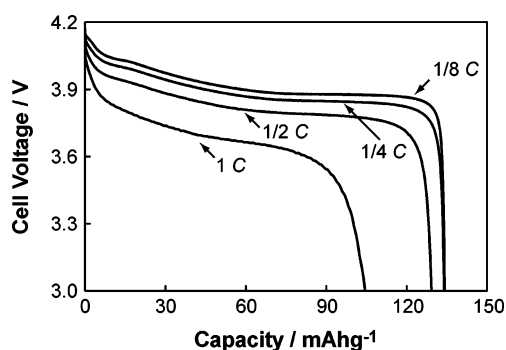
Figure 4. Discharge rate dependencies of discharge curves for a LiCoO$_2$ cathode|DMPImTFSI−LiTFSI mixture electrolyte|lithium metal anode cell.

shows the discharge rate dependencies of the discharge curves of the cell using the DMPImTFSI−LiTFSI mixture electrolyte. Although the discharge voltage decreased in accordance with the discharge rate derived from the IR drop, a notable capacity decrease was not confirmed for up to approximately $^1/_2$ *C*, and

also a high discharge capacity ($>$100 mA h g^{-1}) was obtained for 1 *C*. The lithium ionic conductivity of the DMPImTFSI−LiTFSI mixture electrolyte used in this research might be relatively high as battery electrolyte. The results of this research are very promising because the discharge characteristics at 303 K were very efficient, indicating a promising battery system that is highly safe with a high reversibility. More recently, a new type of anion structure (bis(fluorosulfonyl)imide, FSI) has been reported that achieves low-viscosity and highly conductive room-temperature ionic liquids.[18,19] In this report, although we examined the lithium battery characteristic with cation structural changes, the change in the anion structure is also similarly important for a further characteristic improvement. In the future, we will examine and realize the basic characteristics of batteries using diffusion coefficient measurements (for example, pulsed-gradient spin−echo MNR measurement) and computer simulations and optimize the batteries by changing the chemical structure of room-temperature ionic liquids.

References and Notes

(1) Tarascon, J.-M.; Armand, M. *Nature* **2001**, *414*, 359.
(2) Sakaebe, H.; Matsumoto, H. *Electrochem. Commun.* **2003**, *5*, 594.
(3) Nakagawa, H.; Izuchi, S.; Kuwana, K.; Nukuda, T.; Aihara, Y. *J. Electrochem. Soc.* **2003**, *150*, A695.
(4) Garcia, B.; Lavalle'e, S.; Perron, G.; Michot, C.; Armand, M. *Electrochim. Acta* **2004**, *49*, 4583.
(5) Shin, J.-H.; Henderson, W. A.; Passerini, S. *J. Electrochem. Soc.* **2005**, *152*, A978.
(6) Howlett, P. C.; MacFarlane, D. R.; Hollenkamp, A. F. *Electrochem. Solid-State Lett.* **2004**, *7*, A97.
(7) Seki, S.; Kobayashi, Y.; Miyashiro, H.; Ohno, Y.; Mita, Y.; Usami, A.; Terada, N.; Watanabe, M. *Electrochem. Solid-State Lett.* **2005**, *8*, A577.
(8) Seki, S.; Kobayashi, Y.; Miyashiro, H.; Ohno, Y.; Usami, A.; Mita, Y.; Watanabe, M.; Terada, N. *Chem. Commun.* **2006**, 544.
(9) Hayashi, K.; Nemoto, Y.; Akuto, K.; Sakurai, Y. *J. Power Sources* **2005**, *146*, 689.
(10) Sato, T.; Maruo, T.; Marukane, S.; Takagi, K. *J. Power Sources* **2004**, *138*, 253.
(11) Castriota, M.; Caruso, T.; Agostino, R. G.; Cazzanelli, E.; Henderson, W. A.; Passerini, S. *J. Phys. Chem. A* **2005**, *109*, 92.
(12) Wilkes, J. S.; Zawarotko, M. J. *J. Chem. Soc., Chem. Commun.* **1992**, 965.
(13) Welton, T. *Chem. Rev.* **1999**, *99*, 2071.
(14) Fuller, J.; Carlin, R. T.; Osteryoung, R. A. *J. Electrochem. Soc.* **1997**, *144*, 3881.
(15) Vogel, H. *Phys. Z.* **1921**, *22*, 645.
(16) Fulcher, G. S. *J. Am. Ceram. Soc.* **1923**, *8*, 339.
(17) Seki, S.; Susan, M. A. B. H.; Kaneko, T.; Tokuda, H.; Noda, A.; Watanabe, M. *J. Phys. Chem. B* **2005**, *109*, 3886.
(18) Matsumoto, H.; Sakaebe, H.; Tatsumi, K.; Kikuta, M.; Ishiko, E.; Kono, M. *J. Power Sources*, published online, 2006.
(19) Ishikawa, M.; Sugimoto, T.; Kikuta, M.; Ishiko, E.; Kono, M. *J. Power Sources*, published online, 2006.